THE JOURNAL OF PHYSICAL CHEMISTRY Letters

LETTER

pubs.acs.org/JPCL

Chemisorption-Induced 2D−3D−2D Structural Transitions in Gold Heptamer: $(CO)_nAu_7^-$ (n = 1−4)

Rhitankar Pal,[†] Wei Huang,[‡,⊥] Yi-Lei Wang,[§] Han-Shi Hu,[§] Satya Bulusu,[†,#] Xiao-Gen Xiong,[§] Jun Li,[*,§] Lai-Sheng Wang,[*,‡] and Xiao Cheng Zeng[*,†]

[†]Department of Chemistry, University of Nebraska-Lincoln, Lincoln, Nebraska 68588, United States

[‡]Department of Chemistry, Brown University, Providence, Rhode Island 02912, United States

[§]Department of Chemistry, Tsinghua University, Beijing 100084, China

S Supporting Information

ABSTRACT: CO chemisorption onto the Au_7^- cluster is investigated using photoelectron spectroscopy (PES) and ab initio calculations. It is found that CO binding can induce previously unreported 2D−3D−2D structural changes. The gold motif in the most stable structure of $COAu_7^-$ is an intermediate between the two known stable 2D isomers of Au_7^-. Two minor isomers are observed in the PES of $(CO)_2Au_7^-$; one is due to an unprecedented 3D Au_7^- species with C_s symmetry. This 3D C_s Au_7 motif becomes a major isomer in $(CO)_3Au_7^-$. The most stable isomers of $COAu_7^-$ and $(CO)_2Au_7^-$ are planar with identical Au_7 motifs; the stable planar isomers of $(CO)_3Au_7^-$ include not only the global-minimum structure of Au_7^- but also a planar hexagonal Au_7 motif. The PES spectrum of $(CO)_4Au_7^-$ is markedly different, and its most stable structure consists of the global-minimum structure of Au_7^-, three terminal CO, and one bridging CO.

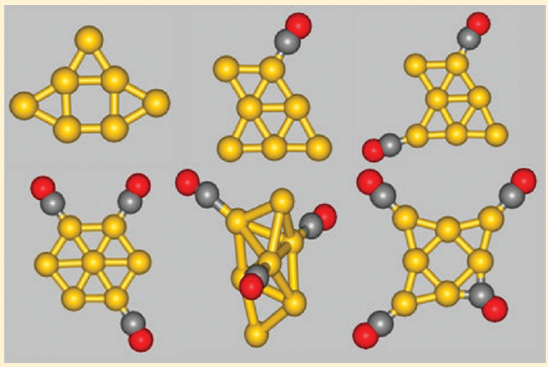

SECTION: Dynamics, Clusters, Excited States

Since the discovery of high catalytic activities for CO oxidation by gold nanoparticles,[1−3] a growing list of important reactions has been found to be catalyzed by gold nanoparticles, such as epoxidation,[4,5] hydrogenation/reduction,[6] C−C bond formation,[7] and water−gas shift.[8] Extensive research has been devoted to the CO oxidation reaction.[9,10] Many factors have been reported to influence the rate of CO oxidation, including cluster size,[11,12] shape, and oxidation/charge state,[13−15] as well as support and methods for preparation of gold nanoparticles.[3,16−18] Numerous models have been proposed, but the exact mechanisms of CO oxidation are still under debate.[3,11−35] Many studies have been focused on CO or O_2 binding to structurally well-defined gold clusters. For example, small-sized gold clusters in anionic,[26] neutral,[27] and cationic[28] states show good CO binding ability. Corner or apex atoms are found to be the preferred sites for the CO binding,[29] for example, on Au_6^-, Au_{16}^-, and Au_{20}.[36−40] In general, gold clusters are capable of binding more than one CO molecules. The binding efficiency can be altered, depending on the flexibility of the geometry.

Previous studies have shown that the gold clusters are usually robust against adsorption of a single CO molecule without major structural transformation,[26,27,36,39,40] although adsorption of multiple COs on gold clusters has been observed to induce significant structural changes.[25,37,38] For example, Au_6^- can maintain its triangular structure even when it binds up to three CO molecules.[36] To our knowledge, there have been few instances where a coinage metal cluster exhibits a significant structural change while binding to a specific ligand. For Au_6^-, for example, we showed in previous studies that chemisorption of at least four CO molecules was required to induce a major structural change.[37] For Ag_5^+, Manard et al. have shown that at least three C_2H_4 molecules are required to induce a major structural change.[41,42] In this Letter, we show experimental and theoretical evidence that the anionic gold heptamer Au_7^- is an unusually flexible cluster; upon binding with 1−4 CO molecules, isomers of the cluster can exhibit 2D to 3D and then back to 2D transitions.

The PES experiments were carried out using a magnetic-bottle-type apparatus equipped with a laser vaporization supersonic cluster source.[43] Briefly, the $(CO)_nAu_7^-$ (n = 1−4) cluster anions were generated using laser vaporization of a pure gold target in the presence of a He carrier gas seeded with 2% CO. $(CO)_nAu_m^-$ clusters were analyzed using a time-of-flight mass spectrometer. The $(CO)_nAu_7^-$ (n = 1−4) clusters of interest were each mass selected and decelerated before being photodetached by a 193 nm (6.424 eV) laser beam. Photoelectrons were collected at nearly 100% efficiency by the magnetic bottle

Received: July 28, 2011
Accepted: August 22, 2011
Published: August 22, 2011

and analyzed in a 3.5 m long electron flight tube. The photoelectron spectra were calibrated using the known spectra of Au^- and Ru^-, and the energy resolution of the apparatus was $\Delta E_k/E_k \approx 2.5\%$, that is, 25 meV for 1 eV electrons.

In the theoretical study, we used the basin-hopping (BH) global search method[44−46] coupled with density functional theory (DFT) to search for low-lying isomers of $(CO)_nAu_7^-$ (n = 1−4). Generalized gradient approximation (GGA) in the Perdew−Burke−Ernzerhof (PBE) functional form was used for the DFT optimization. Multiple structures were used as the initial input for the BH search. After a few hundred BH steps, the program generated a consistent set of a few tens of low-energy isomers for each species. Between 6 and 12 low-lying isomers (typically within 0.3−0.7 eV from the lowest-energy isomer) were used to compute the photoelectron spectra. Next, all low-lying structures were reoptimized at the PBE0/CRENBL level of theory implemented in the NWChem 5.1.1 package,[47] followed by single-point energy calculations at the PBE0/CRENBL level of theory with the inclusion of the spin−orbit (SO) effects for computing the PES spectra. We have recently shown that inclusion of the SO effects can yield nearly quantitative agreement between the experimental and computed PES spectra.[48−52] The first vertical detachment energy (VDE) of an anionic isomer was calculated as the difference between the energy of the neutral and anionic species of each isomer at the corresponding anion geometry. The binding energies of the deeper occupied orbitals of the anion were then added to the first VDE to approximate higher binding energy features. Each computed VDE was fitted with a Gaussian of 0.035 eV width to yield the computed PES spectra. Evidently, the first VDE generated the X peak in the computed spectra shown in Figure 2, and thereafter, the second, third, and fourth VDEs gave rise to A, B, and C peaks, respectively. For several species [$(CO)_2Au_7^-$, $(CO)_3Au_7^-$, and $(CO)_4Au_7^-$], the computed PES spectra of two or more isomers were needed to interpret the experimental data. In these cases, the peaks generated by the minor isomers were labeled as X′, A′, B′, X″, A″, and so forth. Lastly, to examine the relative stability of different isomers, a meta-GGA functional (M06)[53,54] was used with a large basis set (cc-pVTZ-pp).[55,56] It has been recently shown that the M06 functional is very accurate in predicting the relative stability of small-sized gold clusters.[53,54] To confirm the M06 results, the relative stability between the 2D and 3D isomers of $(CO)_nAu_7^-$ (n = 1−4) were also examined at the ab initio coupled cluster level of theory. Indeed, as shown in Table S1 (Supporting Information), the relative stabilities predicted based on the M06 calculations are in very good agreement with those based on the coupled cluster level of theory.

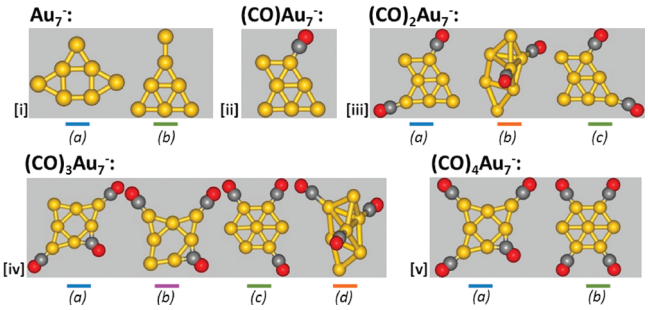

Figure 1. Optimized structures of low-lying isomers of Au_7^- [i], $COAu_7^-$ [ii], $(CO)_2Au_7^-$ [iii], $(CO)_3Au_7^-$ [iv], and $(CO)_4Au_7^-$ [v]. The color bars correspond to those used in the computed spectra in Figure 2 and theoretical VDEs in Table 1.

The Au_7^- cluster has been recently shown to exist as a mixture of two stable isomers in the cluster beam.[49] Both isomers (a) and (b) (Figure 1i) have C_{2v} symmetry. The experimental and computed PES spectra of isomers (a) and (b) are shown in Figure 2i and ii, respectively, for comparisons. The first peak (X) and the third peak

Table 1. Values of the First VDEs Which Correspond to Peaks Marked in the Experimental and Computed Photoelectron Spectra (Figure 2)[c]

		Exp[a]	Theory
	Peaks	VDE (eV)	VDE (eV)
Au_7^-	*X*	3.46 ± 0.02[b]	3.230
	A	4.45 ± 0.03[b]	4.229
	X'	3.92 ± 0.03[b]	3.588
$COAu_7^-$	*X*	3.32	3.169
	A	4.50	4.246
	B	4.68	4.419
$(CO)_2Au_7^-$	*X*	3.08	3.001 3.009
	A	4.11	3.927
	B	4.49	4.283
	X'	3.38	3.306
	A'	3.62	3.575
$(CO)_3Au_7^-$	*X*	2.72	2.681 2.677 2.701
	A	3.85	3.810
	B	4.54	4.403
	X'	3.08	3.065
	A'	3.52	3.454
$(CO)_4Au_7^-$	*X*	2.70	2.723
	A	4.30	4.235
	B	4.58	4.508
	A'	3.99	3.929

[a] Experimental uncertainties are ±0.05 eV, if not specified. [b] From ref 49. [c] The theoretical VDEs are color coded (see color bars in Figure 1) to differentiate isomers.

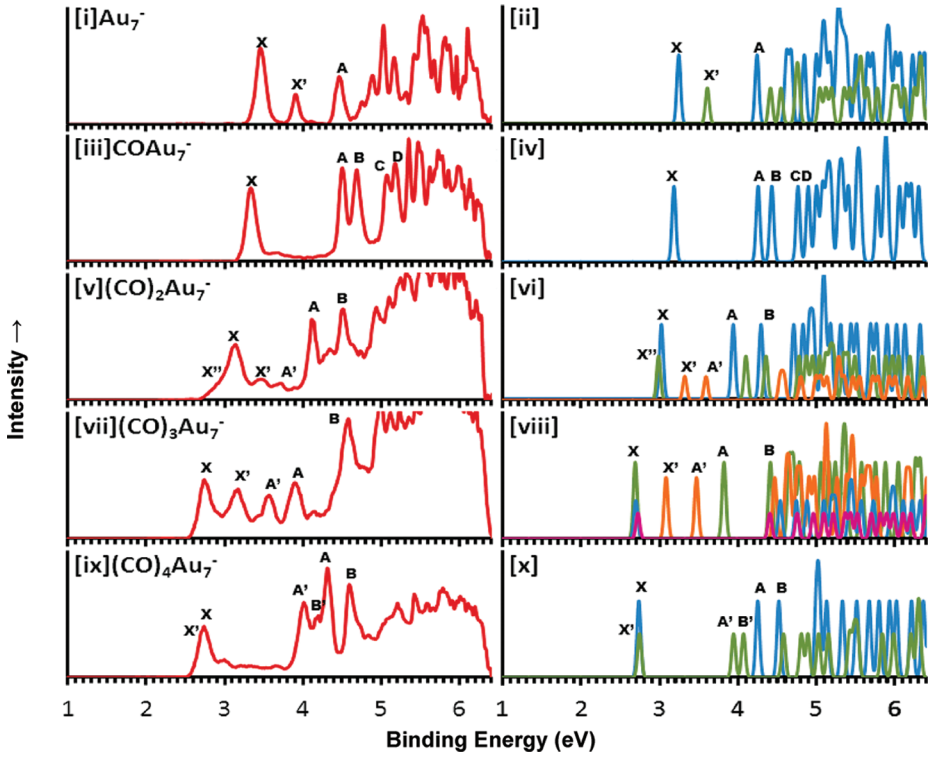

Figure 2. Experimental photoelectron spectra (left panel) and computed photoelectron spectra (right panel) for isomers of Au_7^- [i, ii], $COAu_7^-$ [iii, iv], $(CO)_2Au_7^-$ [v, vi], $(CO)_3Au_7^-$ [vii, viii], and $(CO)_4Au_7^-$ [ix, x]. The color codes in the theoretical PES correspond to those used in the color bars shown in Figure 1 and the theoretical VDEs in Table 1.

(A) in the low-binding-energy region (3.0−4.5 eV) of the experimental spectrum are from the more stable isomer (a); the second peak (X′) represents the first VDE of the minor isomer (b). VDEs of these peaks are given in Table 1.

Upon chemisorption of a single CO, the experimental spectrum of $COAu_7^-$ becomes somewhat simpler (Figure 2iii), suggesting there is only one major isomer present in the cluster beam. The peak X (experimental VDE: 3.32 eV) of $COAu_7^-$ is slightly red-shifted relative to that of Au_7^-. Following a large energy gap, the next two peaks (A and B) are closely spaced at binding energies of ∼4.6 eV. The minor feature X′ present in the spectrum of Au_7^- disappears in the experimental spectrum of $COAu_7^-$. All of these observations suggest that the structure of the $COAu_7^-$ cluster may be significantly different from that of the parent Au_7^-.

Upon binding with two CO molecules, the major peaks (X, A, B) in the spectrum of $(CO)_2Au_7^-$ (Figure 2v) are red-shifted appreciably compared to those of $COAu_7^-$. Moreover, the gap between peaks A and B becomes larger in the spectrum of $(CO)_2Au_7^-$ than in that of $COAu_7^-$. Several minor features (X″, X′, and A′) arise as well, which suggest the presence of minor isomers. Upon adsorption of three CO molecules, the VDE of the peak X in the spectrum of $(CO)_3Au_7^-$ is further red-shifted (Figure 2vii). The PES spectrum of $(CO)_3Au_7^-$ is quite different from that of $(CO)_2Au_7^-$. Noticeably, the minor X′ and A′ features observed in the latter become stronger in the $(CO)_3Au_7^-$ spectrum, resulting in four nearly equally spaced features. This implies the occurrence of two isomers with comparable stabilities. The PES spectrum of $(CO)_4Au_7^-$ (Figure 2ix) looks also very different from that of $(CO)_3Au_7^-$. A wide gap separates the first and second major peaks in the spectrum of $(CO)_4Au_7^-$, suggesting that the minor isomer of $(CO)_3Au_7^-$, responsible for the X′ and A′ peaks, may no longer exist upon binding to the fourth CO. Moreover, the fourth CO does not induce a red shift in the first VDE or the X peak in the spectrum of $(CO)_4Au_7^-$ relative to that in $(CO)_3Au_7^-$.

Scheme 1. Interchange of the Two Major Isomers of Au_7^- (a) and (b), Illustrated to Proceed via an Intermediate Structure (iv)[a]

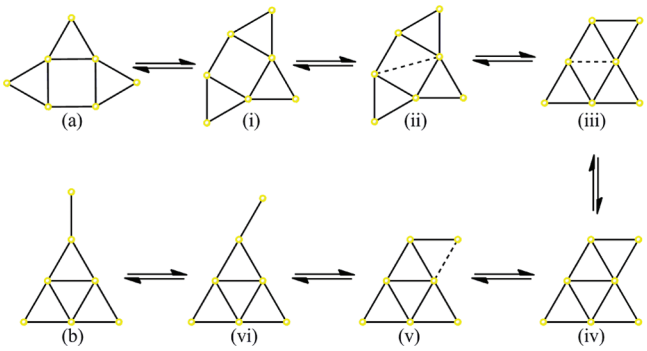

[a] Structures (i), (ii), (iii), (v), and (vi) represent incrementally changed geometries along a transformation pathway. The first CO is adsorbed at the top obtuse corner site of (iv).

Table 1 compares the experimental and theoretical first VDEs for all of the major and minor isomers along with the second or third VDE in some cases. For $COAu_7^-$, the predicted global minimum (Figure 1ii) can reproduce all of the main experimental features (X, A, B, C, D) (see Figure 2iii and iv), providing considerable credence for the identified structure for this

chemisorbed cluster. Furthermore, the computed spectra of several other low-lying isomers of $COAu_7^-$ are given in Figure S1 (Supporting Information). These low-lying isomers can be ruled out because of the poor agreement between the computed spectra and the experimental data or due to their relative high energies (Table S1, Supporting Information). Interestingly, the Au_7 motif in the structure of $COAu_7^-$ is totally different from the two known isomers of Au_7^- [(a) or (b) in Figure 1i]. Thus, the first CO chemisorption induces a major structural change to the Au_7 substrate in $COAu_7^-$ (Figure 1ii). We have identified pathways for the interconversion between the two structures of Au_7^- (a) and (b) and the Au_7 moiety in $COAu_7^-$ (Scheme 1). The intermediate (iv) in Scheme 1, which is the structure of Au_7 in $COAu_7^-$, can be reached from either (a) or (b).

The computed spectra of low-lying isomers of $(CO)_2Au_7^-$ are given in Figure S2 (Supporting Information). Isomer (a) in Figure 1iii reproduces the three main features (X, A, and B) of the experimental spectrum. Hence, it is considered as the major isomer in the cluster beam. A minor feature X″, namely, the long tail to the left of the peak X in the experimental spectrum (Figure 2v) is attributed to the third most stable isomer [(c) in Figure 1iii]. The Au_7 motif of both isomers (a) and (c) in $(CO)_2Au_7^-$ is the same as that in $COAu_7^-$; the two CO molecules bind to the corner sites of the planar Au_7 substrate.[29−36] However, we find that none of the planar isomers of $COAu_7^-$ can reproduce the minor features between peaks X and A in the experimental spectrum. Rather, a 3D isomer with C_s symmetry [(b) in Figure 1iii] is identified, whose computed spectrum nicely reproduces the observed minor features X′ and A′. The energy of the 3D isomer at the SO-PBE0/CRENBL level is slightly higher (0.074 eV) than isomer (a). At the M06/cc-pVTZ-pp level of theory, the 3D C_s isomer (b) is 0.068 eV lower in energy, compared to the lowest-energy 2D isomer. The CCSD(T) calculation further confirms the higher stability of the 3D isomer (b), which is 0.14 eV lower in energy than the most stable 2D isomer (a) (Table S1, Supporting Information). We thus conclude that all three isomers (a)−(c) are likely coexisting in the cluster beam. The observation of the 3D isomer (b) suggests a 2D to 3D structural transition upon chemisorption on Au_7^- by two CO molecules.

The experimental spectrum of $(CO)_3Au_7^-$ is very different from that of $(CO)_2Au_7^-$, indicating emergence of isomers with new structures upon binding with the third CO on Au_7^-. Indeed, the isomers (a), (b), and (c) of $(CO)_3Au_7^-$ [Figure 1iv] possess different 2D structures compared to that of $COAu_7^-$ or $(CO)_2Au_7^-$. Isomer (a) and (b) have identical Au_7 skeletons as the global minimum of the parent Au_7^- [Figure 1i, isomer (a)]. Surprisingly, not all three corner sites are bonded with CO ligands in isomers (a) and (b). Instead, a bridge CO is observed in both isomers. To our knowledge, that a bridged site is preferred over a sharp corner site by a ligand has not been reported in gold clusters, even though CO is largely known to prefer the corner (apex) sites.[29−38] In the case of isomer (c), the Au_7 substrate becomes a hexagon with one central Au. Two CO molecules are bound adjacent to each other in the hexagon (the ortho- and meta-positions), while the third CO is located on the para-position. The fourth isomer (d) [with C_s symmetry] possesses a geometry very similar to the minor 3D isomer (b) of $(CO)_2Au_7^-$. Here, the third CO prefers to occupy a corner site at the same layer that contains the first two CO. The computed first VDEs of isomers (a), (b), and (c) are in good agreement with the experimental X peak (Figure 2vii and viii; Table 1). Isomers (a) and (b) also possess a large gap (>1.7 eV) between the first and second VDE. Isomer (c) has a gap of ∼1.1 eV, which is in excellent agreement with the gap observed between the two strong experimental peaks X and A (Figure 2vii). The computed spectrum of the 3D isomer (d) reproduces nearly perfectly the X′ and A′ features observed in the experimental spectrum. Thus, all the four isomers (a)−(d) must be coexisting, considering the relative intensities of the X, X′, A, and A′ features. The relative abundance of the three planar isomers (a)−(c) cannot be determined because their most characteristic features (X) overlap with each other. However, isomer (d) can be viewed as one of the dominant species as the relative intensities of X′ and A′ are close to those of X and A features. As shown in Table S1 (Supporting Information), at the M06/cc-pVTZ(pp) level, the 3D C_s isomer (d) is about 0.09 eV lower in energy compared to the lowest-lying 2D isomer, whereas at the CCSD(T) level, it is about 0.2 eV lower in energy. We conclude that the 2D isomers (a), (b), and (c) and the 3D isomer (d) of $(CO)_3Au_7^-$ are all present in the cluster beam.

For $(CO)_4Au_7^-$, the predicted global minimum [isomer (a) in Figure 1v; see Table S1, Supporting Information] can reproduce the main experimental peaks X, A, and B quite well. The Au_7 motif of isomer (a) is the same as that of the major isomer of the bare Au_7^- and isomer (a) and (b) of $(CO)_3Au_7^-$. In addition, the minor features, X′ and A′, are found to be best described by the second lowest-lying isomer [(b) in Figure 1v] (Figure S4, Supporting Information), which comes from another contributing isomer (b) of $(CO)_3Au_7^-$. We notice however that there is a very weak peak at about 3 eV binding energy of the experimental spectrum [Figure 2ix]. As shown in Figure S4 (Supporting Information), it is possible that this very weak peak is due to a 3D isomer 3 whose Au_7 skeleton structure may be viewed as a distortion from that of isomer (a). Nevertheless, even though this 3D isomer is present in the cluster beam, its population is extremely small. Indeed, the M06 level of theory shows that the 2D isomers (a) and (b) of $(CO)_4Au_7^-$ are the two lowest-energy isomer (Table S1, Supporting Information). It is indeed a surprise that the 3D isomer similar to isomer (d) of $(CO)_3Au_7^-$ is absent in the population upon adding the fourth CO. One possible explanation for this 3D to 2D transition is that upon adding the fourth CO, the last vacant corner site of the planar isomer (a) or (b) of $(CO)_3Au_7^-$ is now occupied. Hence, the symmetry of the original bare Au_7^- cluster is now recovered due to the full coverage of edge sites by CO molecules, which renders this isomer energetically highly favorable.

In conclusion, our study reveals a number of previously unreported features regarding ligand-binding-induced structural transition in coinage metal clusters. (1) Even with chemisorption of a single CO, a major structural change occurs in Au_7^-. (2) The apex sites in the parent Au_7^- cluster are not always the most preferred sites for the CO chemisorption. (3) A 3D isomer emerges as a minor species in the case of $(CO)_2Au_7^-$, and it becomes one of the major species in the case of $(CO)_3Au_7^-$. Surprisingly, the 3D isomer nearly disappears in the case of $(CO)_4Au_7^-$. This unique 2D−3D−2D structural transition suggests that the Au_7^- cluster is extremely flexible and its structures are strongly dependent on CO chemisorption and coverage. Structural flexibility has been suggested to be important during catalytic reactions. The Au_7^- cluster may be a unique example to study structural flexibility in small 2D gold clusters and how their structures can adapt to different reaction conditions to enable catalytic reactions.

ASSOCIATED CONTENT

Supporting Information. Photoelectron spectra and relative energies for low-lying isomers of $(CO)_nAu_7^-$, Cartesian coordinates of clusters that are relevant to the experiments, and complete ref 47 are collected. This material is available free of charge via the Internet at http://pubs.acs.org.

AUTHOR INFORMATION

Corresponding Author

*E-mail: junli@tsinghua.edu.cn (J.L.); lai-sheng_wang@brown.edu (L.-S.W.); xzeng1@unl.edu (X.C.Z.).

Present Addresses

⊥Anhui Institute of Optics and Fine Mechanics, Chinese Academy of Sciences, Hefei, China.

#Department of Chemistry, York University, 4700 Keele Street, Toronto Ontario, M3J 1P3, Canada.

ACKNOWLEDGMENT

The experimental work was supported by the U.S. NSF (CHE-1049717 to L.-S.W.). The theoretical work done at UNL was supported by grants from the NSF (EPS-1010674) and ARL (W911NF1020099) and by the University of Nebraska's Holland Computing Center, and that done at Tsinghua University was supported by NKBRSF (2011CB932400) and NSFC (20933003) and by the Computer Network Information Center, Chinese Academy of Sciences.

REFERENCES

(1) Haruta, M. Size- and Support-Dependency in the Catalysis of Gold. *Catal. Today* **1997**, *36*, 153–166.

(2) Bond, G. C.; Thompson, D. T. Catalysis by Gold. *Catal. Rev. Sci. Eng.* **1999**, *41*, 319–388.

(3) Haruta, M. When Gold is Not Noble: Catalysis by Nanoparticles. *Chem. Rec.* **2003**, *3*, 75–87.

(4) Nijhuis, T. A.; Visser, T.; Weckhuysen, B. M. A Mechanistic Study Into the Direct Epoxidation of Propene Over Gold−Titania Catalysts. *J. Phys. Chem. B* **2005**, *109*, 19309–19319.

(5) Sinha, A. K.; Seelan, S.; Tsubota, S.; Haruta, M. Catalysis by Gold Nanoparticles: Epoxidation of Propene. *Top. Catal.* **2004**, *29*, 95–102.

(6) McEwan, L.; Julius, M.; Roberts, S.; Fletcher, J. C. Q. A Review of the Use of Gold Catalysts in Selective Hydrogentation Reactions. *Gold Bull.* **2010**, *43*, 298–306.

(7) Tsunoyama, H.; Sakurai, H.; Ichikuni, N.; Negishi, Y.; Tsukuda, T. Colloidal Gold Nanoparticles as Catalyst for Carbon−Carbon Bond Formation: Application to Aerobic Homocoupling of Phenyl Boronic Acid in Water. *Langmuir* **2004**, *20*, 11293–11296.

(8) Bond, G. Mechanism of the Gold-Catalysed Water Gas Shift. *Gold Bull.* **2009**, *42*, 337–342.

(9) Haruta, M.; Tsubota, S.; Kobayashi, T.; Kageyama, H; Genet, M. J.; Delmon, B. Low-Temperature Oxidation of CO over Gold Supported on TiO_2, α-Fe_2O_3 and Co_3O_4. *J. Catal.* **1993**, *144*, 175–192.

(10) Buratto, S. K.; Bowers, M. T.; Metiu, H.; Manard, M.; Tong, X.; Benz, L.; Kemper, P.; Chrétien, S. Au_n and Ag_n (n= 1−8) Nanocluster Catalysts: Gas Phase Reactivity to Deposited Structures. In *The Chemical Physics of Solid Surfaces 12: Atomic Clusters From Gas Phase to Deposited*; Woodruff, D.P., Ed.; Elsevier: Amsterdam, The Netherlands, 2011; pp 151−199, Chapter 4.

(11) Lee, T. H.; Ervin, K. M. Reactions of Copper Group Cluster Anions With Oxygen and Carbon Monoxide. *J. Phys. Chem.* **1994**, *98*, 10023–10031.

(12) Wallace, W. T.; Whetten, R. L. Carbon Monoxide Adsorption on Selected Gold Clusters: Highly Size-Dependent Activity and Saturation Compositions. *J. Phys. Chem. B* **2000**, *104*, 10964–10968.

(13) Wallace, W. T.; Whetten, R. L. Coadsorption of CO and O_2 on Selected Gold Clusters: Evidence for Efficient Room Temperature CO_2 Generation. *J. Am. Chem. Soc.* **2002**, *124*, 7499–7505.

(14) Cox, D. M.; Brickman, R. O.; Creegan, K. In *Clusters and Cluster Assembled Materials*; Averback, R. S., Bernholk, J., Nelson, D. L., Eds.; Mater. Res. Soc. Symp. Proc. No. 206; Materials Reserch Society: Pittsburgh, PA, 1991; p 34.

(15) Bürgel, C.; Reilly, N. M.; Johnson, G. E.; Mitric, R.; Kimble, M. L.; Castleman, A. W., Jr.; Bonačić-Koutecký, V. Influence of Charge State on the Mechanism of CO Oxidation on Gold Clusters. *J. Am. Chem. Soc.* **2008**, *130*, 1694.

(16) Lopez, N.; Norskov, J. K. Catalytic CO Oxidation by a Gold Nanoparticle: A Density Functional Study. *J. Am. Chem. Soc.* **2002**, *124*, 11262–11263.

(17) Socaciu, L. D.; Hagen, J.; Bernhardt, T. M.; Wöste, L.; Heiz, U.; Häkkinen, H.; Landman, U. Catalytic CO Oxidation by Free Au_2^-: Experiment and Theory. *J. Am. Chem. Soc.* **2003**, *125*, 10437–10445.

(18) López-Haro, M.; Delgado, J. J.; Cies, J. M.; Rio, E.; Bernal, S.; Burch, R.; Cauqui, M. A.; Trasobares, S.; Pérez-Omil, J. A.; Bayle-Guillemaud, P.; Calvino, J. J. Bridging the Gap between CO Adsorption Studies on Gold Model Surfaces and Supported Nanoparticles. *Angew. Chem., Int. Ed.* **2010**, *49*, 1981–1985.

(19) Valden, M.; Lai, X.; Goodman, D. W. Onset of Catalytic Activity of Gold Clusters on Titania with the Appearance of Nonmetallic Properties. *Science* **1998**, *281*, 1647–1650.

(20) Chen, M. S.; Goodman, D. W. The Structure of Catalytically Active Gold on Titania. *Science* **2004**, *306*, 252–255.

(21) Lemire, C.; Meyer, R.; Shaikhutdinov, S.; Freund, H. J. Do Quantum Size Effects Control CO Adsorption on Gold Nanoparticles? *Angew Chem., Int. Ed.* **2004**, *43*, 118–121.

(22) Sanchez, A.; Abbet, S.; Heiz., U.; Schneider, W. D.; Häkkinen, H.; Barnett, R. N.; Landman, U. When Gold Is Not Nobel: Nanoscale Gold Catalysis. *J. Phys. Chem. A* **1999**, *103*, 9573–9578.

(23) Yoon, B.; Hakkinen, H.; Landman, U.; Wirz, A. S.; Antonietti, J. M.; Abbet, S.; Heiz, U. Charging Effects on Bonding and Catalyzed Oxidation of CO on Au_8 Clusters on MgO. *Science* **2005**, *307*, 403–407.

(24) Häkkinen, H.; Landman, U. Gas-Phase Catalytic Oxidation of CO by Au_2^-. *J. Am. Chem. Soc.* **2001**, *123*, 9704–9705.

(25) Häkkinen, H.; Abbet, S.; Sanchez, A.; Heiz, U.; Landman, U. Structural, Electronic, and Impurity-Doping Effects in Nanoscale Chemistry: Supported Gold Nanoclusters. *Angew. Chem., Int. Ed.* **2003**, *42*, 1297–1300.

(26) Yuan, D. W.; Zeng, Z Saturated Adsorption of CO and Coadsorption of CO and O_2 on Au_n^- (n = 2−7) Clusters. *J. Chem. Phys.* **2004**, *120*, 6574–6584.

(27) Fernández, E. M.; Ordejón, P.; Balbás, L. Theoretical Study of O_2 and CO Adsorption on Au_n Clusters (n = 5−10). *Chem. Phys. Lett.* **2005**, *408*, 252–257.

(28) Neumaier, M.; Weigend, F.; Hampe, O.; Kappes, M. M. Binding Energies of CO on Gold Cluster Cations Au_n^+ (n = 1−65): A Radiative Association Kinetics Study. *J. Chem. Phys.* **2005**, *122*, 104702.

(29) Zhai, H. J.; Wang, L.-S. Chemisorption Sites of CO on Small Gold Clusters and Transitions from Chemisorption to Physisorption. *J. Chem. Phys.* **2005**, *122*, 051101.

(30) Remediakis, I. N.; Lopez, N.; Nørskov, J. K. CO Oxidation on Rutile Supported Au Nanoparticles. *Angew. Chem., Int. Ed.* **2005**, *44*, 1824–1826.

(31) Wu, X.; Senapati, L.; Nayak, S. K.; Selloni, A.; Hajaligol, M. A Density Functional Study of Carbon Monoxide Adsorption on Small Cationic, Neutral and Anionic Gold Clusters. *J. Chem. Phys.* **2002**, *117*, 4010–4015.

(32) Li, H.; Pei, Y.; Zeng, X. C. Two-Dimensional to Three-Dimensional Structural Transition of Gold Cluster Au_{10} During Soft Landing on TiO_2 Surface and Its Effect on CO Oxidation. *J. Chem. Phys.* **2010**, *133*, 134707.

(33) Varganov, S. A.; Olson, R. M.; Gordon, M. S.; Meitu, H. The Interaction of Oxygen With Small Gold Clusters. *J. Chem. Phys.* **2003**, *119*, 2531–2537.

(34) Fielicke, A.; von Helden, G.; Meijer, G.; Simard, B.; Rayner, D. M. Gold Cluster Carbonyls: Vibrational Spectroscopy of the Anions and the Effects of Cluster Size, Charge, and Coverage on the CO Stretching Frequency. *J. Phys. Chem. B* **2005**, *109*, 23935–23940.

(35) Kimble, M. L.; Castleman, A. W., Jr.; Mitric, R.; Bürgel, C.; Bonačić-Koutecký, V. Reactivity of Atomic Gold Anions toward Oxygen and Oxidation of CO: Experiment and Theory. *J. Am. Chem. Soc.* **2004**, *126*, 2526–2535.

(36) Zhai, H. J.; Kiran, B.; Dai, B.; Li, J.; Wang, L.-S. Unique CO Chemisorption Properties of Gold Hexamer: $Au_6(CO)_n^-$ (n = 0−3). *J. Am. Chem. Soc.* **2005**, *127*, 12098–12106.

(37) Zhai, H. J.; Pan, L. L.; Dai, B.; Kiran, B.; Li, J.; Wang, L.-S. Chemisorption-Induced Structural Changes and Transition from Chemisorption to Physisorption in $Au_6(CO)_n^-$ (n = 4−9). *J. Phys. Chem. C* **2008**, *112*, 11920–11928.

(38) Yang, X.-F.; Wang, Y.-L.; Zhao, Y.-F.; Wang, A.-Q.; Zhang, T.; Li, J. Adsoption-Induced Structural Changes of Gold Cations From Two- to Three- Dimensions. *Phys. Chem. Chem. Phys.* **2010**, *12*, 3038–3043.

(39) Li, J.; Li., X.; Zhai, H.-J.; Wang, L.-S. Au_{20}: A Tetrahedral Cluster. *Science* **2003**, *299*, 864–867.

(40) Huang, W.; Bulusu, S.; Pal, R.; Zeng, X. C.; Wang, L.-S. CO Chemisorption on the Surfaces of the Golden Cages. *J. Chem. Phys.* **2009**, *131*, 234305.

(41) Manard, M. J.; Kemper, P. R.; Bowers, M. T. Probing the Structure of Gas-Phase Metallic Clusters via Ligation Energetics: Sequential addition of C_2H_4 to Ag_m^+ (m = 3−7). *J. Am. Chem. Soc.* **2005**, *127*, 9994–9995.

(42) Manard, M. J.; Kemper, P. R.; Bowers, M. T. An Experimental and Theoretical Investigation Into the Binding Interactions of Silver Cluster Cations with Ethene and Propene. *Int. J. Mass. Spectrom.* **2006**, *249−250*, 252–262.

(43) Wang, L. S.; Cheng, H. S.; Fan, J. W. Photoelectron Spectroscopy of Size-Selected Transition Metal Cluster: Fe_n^- (n = 3−24). *J. Chem. Phys.* **1995**, *102*, 9480–9493.

(44) Wales, D. J.; Doye, J. P. K. Global Optimization by Basin Hopping and the Lowest Energy Structures of Lenard-Jones Clusters Containing up to 110 Atoms. *J. Phys. Chem. A* **1997**, *101*, 5111–5116.

(45) Yoo, S.; Zeng, X. C. Global Geometry Optimization of Silicon Clusters Described by Three Empirical Potentials. *J. Chem. Phys.* **2003**, *119*, 1442–1450.

(46) Yoo, S.; Zeng, X. C. Motif Transition in Growth Patterns of Small to Medium-Sized Silicon Clusters. *Angew. Chem., Int. Ed.* **2005**, *44*, 1491–1494.

(47) Bylaska, E. J. et al. *NWCHEM, A Computational Chemistry Package for Parallel Computers*, version 5.1.1; Pacific Northwest National Laboratory: Richland, WA.

(48) Huang, W.; Bulusu, S.; Pal, R.; Zeng, X. C.; Wang, L. S. Structural Transition of Gold Nanoclusters: From the Golden Cage to the Golden Pyramid. *ACS Nano* **2009**, *3*, 1225–1230.

(49) Huang, W.; Pal, R.; Wang, L. M.; Zeng, X. C.; Wang, L. S. Isomer Identification and Resolution in Small Gold Clusters. *J. Chem. Phys.* **2010**, *132*, 054305.

(50) Wang, Y.-L.; Zhai, H.-J.; Xu, L.; Li, J.; Wang, L. S. Vibrationally-Resolved Photoelectron Spectroscopy of Di-Gold Carbonyl Clusters $Au_2(CO)_n^-$ (n = 1−3): Experiment and Theory. *J. Phys. Chem. A* **2010**, *114*, 1247.

(51) Wang, L. M.; Pal, R.; Huang, W.; Zeng, X. C.; Wang, L. S. Observation of Earlier Two-to-Three Dimensional Structural Transition in Gold Cluster Anions by Isoelectronic Substitution: MAu_n^- (n = 8−11, M = Ag, Cu). *J. Chem. Phys.* **2010**, *132*, 114306.

(52) Pal, R.; Wang, L. M.; Huang, W.; Wang, L. S.; Zeng, X. C. Structure Evolution of Gold Cluster Anions Between The Planar and Cage Structures by Isoelectronic Substitution: Au_n^- (n = 13−15) and MAu_n^- (n = 12−14, M = Ag, Cu). *J. Chem. Phys.* **2011**, *134*, 054306.

(53) Mantina, M.; Valero, R.; Truhlar, D. G. Validation Study of the Ability of Density Functionals to Predict the Planar-to-Three-Dimensional Structural Transition in Anionic Gold Clusters. *J. Chem. Phys.* **2009**, *131*, 064706.

(54) Ferrighi, L.; Hammer, B.; Madsen, G. K. H. 2D−3D Transition for Cationic and Anionic Gold Clusters: A Kinetic Energy Density Functional Study. *J. Am. Chem. Soc.* **2009**, *131*, 10605–10609.

(55) Dunning, T. H., Jr. Gaussian Basis Sets for Use in Correlated Molecular Calculations. I. The Atoms Boron through Neon and Hydrogen. *J. Chem. Phys.* **1989**, *90*, 1007–1023.

(56) Peterson, K. A.; Puzzarini, C. Systematically Convergent Basis Sets for Transition Metals. II. Pseudopotential-Based Correlation Consistent Basis Sets for the Group 11 (Cu, Ag, Au) and 12 (Zn, Cd, Hg) Elements. *Theor. Chem. Acc.* **2005**, *114*, 283.